Regularized reconstruction of 3D high-resolution magnetic resonance images from acquisitions of anisotropically degraded resolutions.

Elodie Roullot[1,2]   Alain Herment[2]   Isabelle Bloch[1]   Mila Nikolova[1]   Elie Mousseaux[2,3]

[1] ENST Département TSI
46, rue Barrault, 75013 Paris, France
Elodie.Roullot@enst.fr

[2] INSERM U494, Université Paris VI, France

[3] CIERM, Université Paris XI, France

Abstract

We present an original method to reconstruct three-dimensional magnetic resonance images of high resolution in the 3 directions of space from two anisotropic volumes. The resolution of each volume is degraded in a different direction. The reconstruction method is based on an optimization technique, the constraints being fidelity to the acquired data on the one hand, smoothness and edge preservation on the other hand. The interest of such a method is to significantly decrease the acquisition time of MR images, without degrading the spatial resolution.

1. Introduction

Reconstruction of a high resolution image from a series of undersampled images in order to overcome the limited resolution of the acquisition system is a subject of great interest for many authors; usually the methods consist in acquiring the scene with subpixel displacements [4], or with different incidence angles [5].

As opposed to many applications of high resolution image restoration, in Magnetic Resonance Imaging (MRI) the limit is not due to the acquisition system resolution but rather to the acquisition time. For example, the patient is often required to hold his/her breath during the acquisition; besides, when working on substracted images (difference between images acquired with and without injection of contrast medium into the vessels), the slightest movement of the patient causes motion artifacts in the substracted image.

Acquisition time and resolution are intrinsically linked in MRI [8], so the constraint of time limit comes down to a constraint of resolution.

That is why fast acquisition sequences such as "fast gradient echo" have been developed; unfortunately they cannot be applied to angiography.

Our study is based on an original acquisition process, consisting of two series of orthogonal slices with different directions of anisotropy, and presented in Section 2. Our aim is the reconstruction of an isotropic volume, complying with some criteria such as edge preservation and smoothness of homogeneous areas, for applications in segmentation and quantization of vascular structures.

The degradation process is mathematically described in Section 3. Section 4 is dedicated to our reconstruction method. Some examples are presented in Section 5.

2. Acquisition process

In this part we will describe the acquisition principles; for more details about MRI acquisition, refer to [1, 8].

First of all we shall recall the basics of MRI: in one dimension, the acquired signal (called FID: free induction decay) can be expressed as the superposition of many signals produced by individual voxels, the frequency of each being proportional to the spatial location of the corresponding voxel; this principle is called "frequency encoding". In three dimensions, signal localization uses frequency encoding in one direction, and two types of "phase encoding" in the other directions. Thus, the signal received is the 3D Fourier transform of the image we are looking for.

The time required for acquiring a volume of dimensions N_x, N_y and N_z respectively in the directions of frequency encoding and of both phase encodings is:

$$T = N_y \cdot N_z \cdot T_R$$

where T_R is the so-called "repetition time" [8]. This expression shows well the trade-off between resolution and acquisition time in MRI, excepted in the direction of frequency encoding.

We propose to acquire two anisotropic volumes with orthogonal slice directions, each of them having a high resolution in both directions of the slice, and a degraded resolution

346

in the orthogonal direction. The method thus consists in re-constructing from both volumes a unique volume of high resolution in all directions.

The principle is shown in a more schematic way in Figure 1: from the acquired data (sagittal and axial slices), two anisotropic frontal volumes are computed, from which we reconstruct one unique high resolution frontal volume. See Figures 3 and 5 for examples of corresponding anisotropic slices.

Let N_x, N_y and N_z be the dimensions along the x, y and z axes of the volume to reconstruct. The time required to acquire the first volume, with a degraded resolution along y (thus of dimensions N_x, N_y', N_z, with $N_y' < N_y$), followed by the second volume, with a degraded resolution along x (thus of dimensions N_x', N_y, N_z) is:

$$T_{s+a} = T_R \cdot N_z \cdot N_y' + T_R \cdot N_z \cdot N_x'.$$

Acquiring directly the frontal volume with a high resolution would have led to an acquisition time of:

$$T_f = T_R \cdot N_z \cdot N_y.$$

Therefore, time can be saved if:

$$N_y' + N_x' < N_y.$$

For example, if $N_x = N_y$ and $N_x' = N_y' = N_x/3$, we have saved a relative time amount of 33 % in comparison with a unique high resolution acquisition.
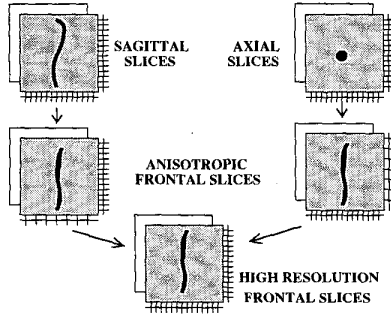

Figure 1. Schematic problem statement.

3. Modeling of the degradation

The three-dimensional reconstruction problem presented above reduces to a two-dimensional problem, since we can process each couple of corresponding slices independently.

Let I be the high resolution image ($N_y \times N_x$) we are looking for. Would we acquire directly this image, then the acquired data would be its 2D Discrete Fourier Transform (DFT) (see Section 2) which we can express as:

$$DFT(I) = \frac{1}{N_x \cdot N_y} F_y \cdot I \cdot F_x,$$

the $N_y \times N_y$ matrix $\frac{1}{N_y} F_y$ being the DFT operator working on the columns, and the $N_x \times N_x$ matrix $\frac{1}{N_x} F_x$ being the DFT operator working on the rows, with:

$$F_y(m,n) = e^{-j \cdot 2\pi \cdot m \cdot n / N_y}, \text{ with } m,n = 0...N_y - 1,$$

$$F_x(m,n) = e^{-j \cdot 2\pi \cdot m \cdot n / N_x}, \text{ with } m,n = 0...N_x - 1.$$

Now let us express I_x and I_y, the two images with degraded resolutions respectively along x and y, as functions of I.

Note that we use "zero-padding" to work with constant image sizes; this is equivalent to interpolating the low resolution images. Also note that for symmetry considerations we work with even image dimensions (N_x and N_y as well as N_x' and N_y'). Thus:

$$DFT(I_x) = \frac{1}{N_x \cdot N_y} F_y \cdot I \cdot F_x \cdot M_x,$$

$$DFT(I_y) = \frac{1}{N_x \cdot N_y} M_y \cdot F_y \cdot I \cdot F_x,$$

where M_y and M_x are diagonal matrices of sizes $N_y \times N_y$ and $N_x \times N_x$ respectively:

$$\begin{cases} M_{ii} = 0 & \text{if } N_t \le i \le N - N_t \\ M_{ii} = 1 & \text{else,} \end{cases}$$

with (in direction x for example):

$$N_t = \frac{N_x'}{2} + 1$$

corresponding to the reduced truncature frequency, and i varying from 0 to $N_x - 1$ (in the example of direction x) with the convention that reduced frequencies in the DFT vary from 0 to 1. Thus, $N_x F_x^{-1}$ and $N_y F_y^{-1}$ being the IDFT operators:

$$I_x = N_y F_y^{-1} \cdot DFT(I_x) \cdot N_x F_x^{-1} = I \cdot F_x \cdot M_x \cdot F_x^{-1},$$

and in the same way:

$$I_y = F_y^{-1} \cdot M_y \cdot F_y \cdot I.$$

In the following we will use the degradation operators D_x and D_y defined as:

$$D_x = F_x \cdot M_x \cdot F_x^{-1},$$

$$D_y = F_y^{-1} \cdot M_y \cdot F_y.$$

4. Regularized reconstruction

In order to satisfy on the one hand, a good signal to noise ratio as well as edge preservation, and on the other hand, a good adequation to the data contained in both input images, we propose to minimize an energy functional taking into account each of these constraints. This approach has been studied in many papers [3, 2].

4.1. The energy functional

The energy functional has the following form:

$$J = Q + \lambda \cdot \Phi$$

where λ allows a trade-off between Φ, the regularization term, and Q, the fidelity to the data. Both terms are described below.

Fidelity to the data:

The matter is to minimize the sum of the quadratic errors between the reconstructed image and the data:

$$Q = \| I_{rec} \cdot D_x - I_x \|^2 + \| D_y \cdot I_{rec} - I_y \|^2$$

where D_x and D_y are the operators of resolution degradation as in Section 3, $\| \cdot \|$ represents the $\mathcal{L}^2$ norm, I_{rec} is the high resolution image at current iteration, I_x and I_y are the low resolution input images.

Regularization term:

It takes the following form:

$$\Phi = \sum_{i=1}^{N_x} \sum_{j=1}^{N_y} (\psi((I_{rec} \cdot \Delta_x)_{i,j}) + \psi((\Delta_y \cdot I_{rec})_{i,j}))$$

where ψ is a potential function, and Δ_x and Δ_y are the operators of neighbor differences along directions x and y.

We choose to use the Huber potential function [2] (Figure 2) which, when applied to the first order neighbor differences, smoothes the areas with small local differences while preserving discontinuities at the sites with higher local differences:

$$\begin{cases} \psi(x) = x^2 & \text{si } | x | \le \alpha \\ \psi(x) = 2 \cdot \alpha \cdot | x | - \alpha^2 & \text{si } | x | > \alpha \end{cases}$$

The influence of parameter α was studied in [6]; intuitively, when α is small, edges are better preserved, while when α is greater, edges are smoothed as with the quadratic function.
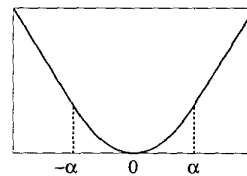

Figure 2. The Huber potential function.

Convexity:

We proved in [7] that the energy functional is convex but not strictly, so there may be several solutions minimizing the functional, forming a connected set.

4.2. Optimization method

We choose a deterministic method well-suited for minimizing convex energies: the well-known conjugate gradient method. Since our functional is not strictly convex, great attention should be paid to the initialization: for example we can choose the average between both acquisitions.

5. Experimental results

We show here the results obtained for two sample slices of one of the several patient volumes we processed (due to lack of place the MIPs (Maximum Intensity Projections) cannot be shown here). From the sagittal and the axial volumes we compute the corresponding frontal volumes (shown for our two sample slices in Figures 3 and 5), with a resolution of 4 mm in x and 0.98 mm in y for the sagittal volume and with a resolution of 0.98 mm in x and 4 mm in y for the axial volume. Then we reconstruct a unique high resolution volume; Figures 4 and 6 show the results corresponding to Figures 3 and 5.
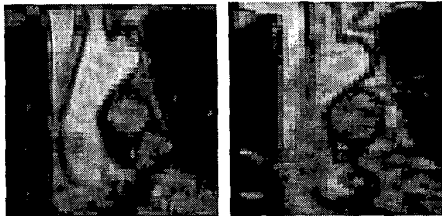

Figure 3. A couple of anisotropic frontal slices of the aorta, computed from the sagittal volume (left) and from the axial volume (right).

These results were visually evaluated by an expert, who judged the final regularized result better than the low resolution acquisitions and than the non-regularized results.
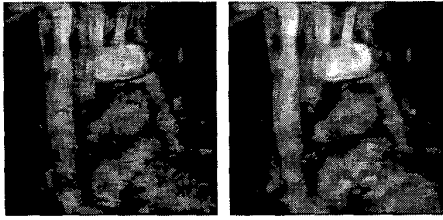
Figure 4. Results obtained from the slices of Figure 3. left: $\lambda \simeq 0$; **right:** $\lambda = 2$ **and** $\alpha = 0.005$.

Figure 5. A couple of anisotropic frontal slices of the aorta, computed from the sagittal volume (left) and from the axial volume (right).
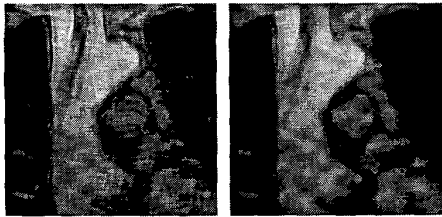
Figure 6. Results obtained from the slices of Figure 5. left: $\lambda \simeq 0$; **right:** $\lambda = 2$ **and** $\alpha = 0.005$.

Moreover, the method was quantitatively evaluated on a physical vessel phantom of high resolution with known dimensions, from which the degraded acquisitions were simulated. The method proved to be robust against noisy data, as well as against small changes of parameters α and λ; edges were quantitatively compared to original edges and proved to be well-preserved.

6. Conclusion and future work

We have presented a reconstruction method taking into account both fidelity to the acquired data, and an edge preserving regularization criterion. This method is based on an original acquisition process composed of two anisotropic volumes. It allows to reduce the acquisition time in MRI without degrading the spatial resolution. Convexity of the criterion makes the conjugate gradient algorithm convenient for minimization; moreover, the methods proved to be robust against the parameters as well as against noisy data (see [7]). Medical experts judged the method to give at least as good results as a unique high resolution acquisition.

We consider several tracks for future work: first of all, a judicious choice of the regularization parameter allows to obtain either a visually good result (reasonable regularization), or an easily segmentable result (high regularization), this last case being of high interest for our long-term goal: quantization of vessel dimensions. We also consider to extend the regularization to the third dimension (the constant resolution dimension) in order to improve robustness against noisy data; finally, we may also extend the acquisition process to three acquisitions, i.e. by adding a third anisotropic acquisition with low resolution along the third dimension.

References

[1] J. Bittoun. Basic Principles of Magnetic Resonance Imaging. In S. Cerdan, A. Haase, and F. Terrier, editors, *SYLLABUS - Methodology, Spectroscopy and Clinical MRI*, pages 45–52. ESMRMB, Springer-Verlag, September 1998.

[2] M. J. Black and A. Rangarajan. On the Unification of Line Process, Outlier Rejection, and Robust Statistics with Applications in Early Vision. *International Journal of Computer Vision*, 19(1):57–91, 1996.

[3] D. Geman and G. Reynolds. Constrained Restoration and the Recovery of Discontinuities. *IEEE Transactions on Pattern Analysis and Machine Intelligence*, 14(3):367–383, March 1992.

[4] M. Irani and S. Peleg. Improving Resolution by Image Registration. *Graphical Models and Image Processing*, 53(3):231–239, May 1991.

[5] T. Komatsu and T. Igarashi. Very High Resolution Imaging Scheme with Multiple Different-Aperture Cameras. *Signal Processing: Image Communication*, 5:511–526, 1993.

[6] M. Nikolova. Local Strong Homogeneity of a Regularized Estimator. *SIAM Journal of Applied Mathematics*, 1999. (to appear).

[7] E. Roullot, A. Herment, I. Bloch, M. Nikolova, and E. Mousseaux. Reconstruction régularisée d'images de résonance magnétique 3D de haute résolution à partir d'acquisitions de résolutions anisotropes. In *Actes du 12ème congrès AFCET-AFIA Reconnaissance de Formes et Intelligence Artificielle (RFIA'2000)*, volume 2, pages 59–68, Paris, France, February 2000. ENST.

[8] G.A. Wright. Magnetic Resonance Imaging. *IEEE Signal Processing Magazine*, pages 56–66, January 1997.